COMPARISON OF MODULE TEMPERATURE MEASUREMENT METHODS

Stefan Krauter, Alexander Preiss

Photovoltaik Institut Berlin AG
Einsteinufer 25, D-10587 Berlin, Germany
Phone: +49 30 314 25977, Fax: +49 30 314 26617
krauter@pi-berlin.com, www.pi-berlin.com

ABSTRACT

Aim of this study is to improve the prediction of electrical energy yield especially for PV modules based on thin film technologies. Problems with deficient power prediction of PV power plants have manifold reasons: One of the easy accessible is the measurement of NOCT (nominal operation cell temperature). Deviations of NOCTs measured have a direct influence of the yield predicted (1–5%). The deviations due to different measurement methods and different temperature sensors have been discussed in theory (systematic error) and have been investigated in laboratory tests as well as under real world conditions in an outdoor lab. The thermal behavior is studied and the measurement results are compared to theoretical models. As a result the theoretical yield as a function of the measured NOCT is compared for different installation sites and for different technologies.

INTRODUCTION & BACKGROUND

The empiric method to determine the relevant module temperature (or better: the temperature of the *p-n* junction) leads to the NOCT (nominal operation cell temperature).
The NOCT is defined as the temperature of a PV module at the Standard Reference Environment (SRE): Irradiance of 800 W/m^2, ambient temperature of 20°C, wind speed of 1 m/s, no electrical load, oriented towards South and at an inclination angle of 45°.
The IEC 61215/61646 norms specify the measurement method to determine that temperature. The temperature of the module (T_c) minus the ambient temperature (T_a) is interpolated for a minimum irradiance range of 300 W/m^2 above a minimum irradiance of 400 W/m^2.

$$NOCT = (T_C - T_a)_{SRE} + 20°C \qquad (1)$$

Hence the recommended test conditions are rare and at the end not sufficiently determined by the norm, the NOCTs measured can be found in a range of almost ±5K, mainly caused by an undefined ratio of diffuse and direct irradiance.

The effect of the operating temperature on the efficiency of a module as well as on the electrical yield depends on the absolute temperature coefficients of mainly voltage β and less current α.

$$I_{SC\ corr} = I_{SC} + \alpha(T_2 - T_1) \qquad (2)$$

$$V_{OC\ corr} = V_{OC} + \beta(T_2 - T_1) \qquad (3)$$

These coefficients have been measured in a sun simulator under laboratory conditions. The *I-V*-curves of the heated modules are measured for temperatures in the vicinity of 50°C. The values for *β, α* have been interpolated from this measurement. Typical values are listed in Table 1.

Table 1. Average temperature coefficients from *Photon Magazine* (Photon Market Survey 2008).

Technology	***β TC*** in V/K	***α TC*** in A/K
c-Si (mono)	-0.00364512	0.00046915
c-Si (multi)	-0.0037199	0.00047709
a-Si	-0.00327806	0.00074003

The power output *P* is mainly a function of the module temperature and irradiance *P(T,G)*, neglecting the spectral effects in this case. Therefore it is necessary to calculate the thermal equilibration of a module under real world conditions. This can be quite complex, implicit heat transfer functions describing mechanisms like wind induced and natural convection as well as radiation effects. It is necessary to know physical material parameters of the module layers and the pertinent mounting of the test specimen has to be known as well [1].

Another approach is an empiric one, to calculate or extrapolate the temperature of the module from measured data. The simplest formula to calculate the cell temperature was investigated by Ross [3]:

$$T_C = T_a + \kappa \cdot G \qquad (4)$$

That simple linear connection of cell temperature, ambient temperature, irradiance respectively and a constant (κ: Ross coefficient) depending on the mounting structure gives a first orientation. But to determine the Ross coefficient in before is nearly impossible, there are some measured values listed in Table 2.

Table 2. Empiric Ross-coefficients [3].

Mounting type	**κ** (K·m²/W)
Free standing	0.021
Flat roof	0.026
Sloped roof: well cooled	0.020
Sloped roof: highly integrated	0.056

The relation to determine the cell temperature from NOCT is derived from a simple approach of a steady state electrical yield prediction.

$$\eta \cdot G = (\tau \cdot \alpha) \cdot G - U(T_C - T_a) \tag{5}$$

$$T_C = T_a + \left(\frac{G}{G_{NOCT}}\right)\left(\frac{U}{U_{NOCT}}\right)(T_{NOCT} - T_a)\left(1 - \frac{\eta}{\alpha\tau}\right) \tag{6}$$

G	irradiance in module plane
η	PV conversion efficiency

U is a constant depending on irradiance for the thermal losses, in that simple model not depending on e.g. wind speed; τ transmittance of glazing; α absorbance of PV layer.

To calculate the temperature from NOCT some further assumptions have been made: $\eta=0$ and as a simplification U as constant leads to:

$$T_C = T_a + \left(\frac{T_{NOCT} - T_a}{G_{NOCT}}\right) \cdot G \tag{7}$$

To overcome the problem of the heat transfer whereas the influence of wind induced heat transfer is the main point, [4] proposes a similar simple but wind depending expression of T_c:

$$T_C = T_a + \left(\frac{0.32}{8.91 + 2v_W}\right) \cdot G\,; \quad v_W > 0 \tag{8}$$

That expression derives from an assumption that radiation as well as natural convection heat transfer are minor effects and can be neglected, and a standard NOCT value is around 46°C.

TEMPERATURE MEASUREMENT

As described the electrical yield depends on the irradiance but is directly influenced by the temperature. The most interesting temperature on a module is in fact the one of the *p-n* junction. The I_{sc} (short circuit current) can be considered as nearly independent on T (because of minuscule values for temperature coefficient α) and just be a function on G (not for thin film modules, which differs in the weak light behavior). It increases with higher temperatures which can be explained with an increased absorption caused by decreasing band gap. The V_{oc} (open circuit voltage) is much more sensitive for temperature and decreases as well as the efficiency η and Fill Factor *FF*:

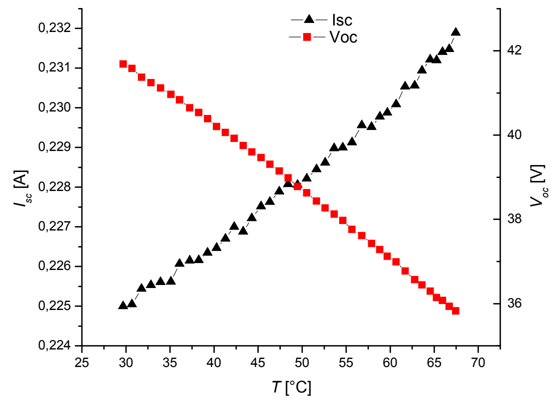

Fig. 1. Short circuit current I_{SC} (black) and open circuit voltage V_{OC} (red) as a function of module temperature T. Measurements have been carried out to extrapolate the temperature coefficients for voltage and current.

To determine the junction temperature according to IEC 60904-5 it is necessary to have the temperature coefficient β for the voltage and to have weak light measurements.

$$T_2 = T_1 + \beta^{-1}\left(V_{OC2} - V_{OC1} + D\frac{1}{ns}\ln\left(\frac{G_1}{G_2}\right)\right) \tag{9}$$

In that expression D is the thermal voltage and has to be measured in two additional weak light tests; ns is the number of cells in series.

To improve accuracy temperature measurements and NOCT determination have to be carried out precisely due to the negative temperature coefficients for PV power generation. However, we found significant deviations for the different practices of temperature measurements and determinations. The following article compares the six different methods to determine the operating temperature of a PV module:

1. Determination of junction temperature via the open-circuit voltage of the cell.
2. Cell temperature measurement via cell-attached Pt-100 foil-sensors, laminated inside the module.
3. Surface measurements via attached Pt-100 sensors (with and without heat conductive paste).
4. Surface measurements via an attached Pt-100 sensor with different thickness of layers of fixation tape to prevent cooling of sensor from ambient.

5. Surface measurements via a thermo-graphic camera (with and without setting the thermal emission coefficient of the surface)

6. Additionally we found that unqualified ambient temperature measurement can lead to deviations of ±2 K even using accurate temperature sensors.

APPROACH & RESULTS

A preliminary screening of inaccuracies has been carried out. The results of that screening are presented in Table 3.

Table 3. Overview (first estimate) on parameters that influence PV yield prediction (see [5]).

Parameter	**Accuracy of data available (±)**	**Effect on PV yield (±)**
Irradiance: horizontal global irradiance	2-4%	2-4%
tilted global irradiance	3-5%	3-5%
actual spectral information	10-70%	20%
Polarization	20%	0.5-1%
Albedo	2%	0.5%
Outdoor temperature	2%	0.5%
Wind speed	50%	1.5%
wind direction (at module)	10%	1%
refractive indices	2%	0.5-1%
absorption coefficients	2-10%	0.5 %
Heat conductivity of module materials	3-10%	0.5-1%
spectral response	5-10%	5-10%
Temperature coefficients	5-20%	5-20%
weak light performance	20%	20%
degradation (for thin film modules)	20%	20%
heat exchange	2-5%	0.7%
Emissivity of ground surfaces	10-15%	0.5%
Sky temperature	15-20%	0.5%
Natural convection		
Forced convection		
MPP tracking accuracy	0.5-1%	0.5-1%
Measurement of electrical power output and yield	0.5-1%	0.5-1%

However, starting with the measurement of NOCT as described above. In field measurement we determined with different sensors according to IEC 61215/61646 NOCT values. The results are shown in Fig. 7 and are listed in Table 5.

As can be seen in Fig. 2 the sensors are attached on the PVF-backsheet of a standard sized c-Si module. One of the sensors is laminated inside the module attached directly to the backside of one c-Si cell. First step was to study the heat-up behavior and response of the sensors in a steady state sun light simulator.

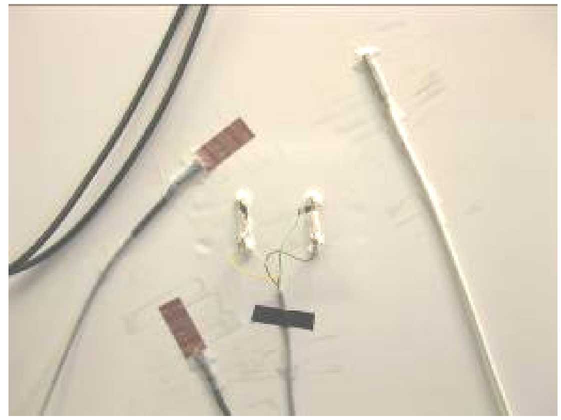

Fig. 2. The temperature sensors on the backside of the backsheet of a glass-Tedlar® module.

The resulting thermal behavior is plotted in Fig. 3, Fig. 4 and in Fig. 5. The corresponding sensors are listed in Table 5.

THEORETICAL CONSIDERATIONS

The temperature difference between the solar cell and the surface can be calculated via a simple heat conduction equation:

$$T_{Cell} - T_{Surface} = \left(\frac{\dot{Q}}{\sum R_{therm}} \right) \quad (10)$$

for a glass-glass-module:

$$\sum R_{therm\,back1} = R_{EVA} + R_{Glass} = \left(\frac{d_{EVA}}{k_{EVA}} \right) + \left(\frac{d_{Glass}}{k_{Glass}} \right) \quad (11)$$

for a glass-Tedlar®-module, the thermal resistance to the front is the same as for the glass-glass module, but towards the back surface:

$$\sum R_{therm\,back2} = R_{EVA} + R_{Tedlar} = \left(\frac{d_{EVA}}{k_{EVA}} \right) + \left(\frac{d_{Tedlar}}{k_{Tedlar}} \right) \quad (12)$$

applying the adequate thicknesses of
d_{EVA} = 0.5 mm, d_{Glass} = 4 mm, d_{Tedlar} = 0.15 mm and also the thermal conductivities of
k_{EVA} = 0.34 W/(m²·K), k_{Glass} = 1.0 W/(m²·K), and
k_{Tedlar} = 0.167 W/(m²·K)

for a heat flux *Q/t* of 400 W/m² to the backside of the module (a total heat flux of 800 W/m² roughly divided equally in a flux to the front and in a flux to the backside): the temperature difference between the junction and the module surface is (for the back surface of a glass-glass module):

$$T_{solar\,cell} - T_{back\,surface} = 2.19\text{ K}$$

and for the back surface of a glass-Tedlar® module:

$$T_{solar\ cell} - T_{back\ surface} = 0.95\ \mathrm{K}$$

Those temperature differences are methodical imprecisions of that kind of temperature measurements and occur independently from the sensor applied.

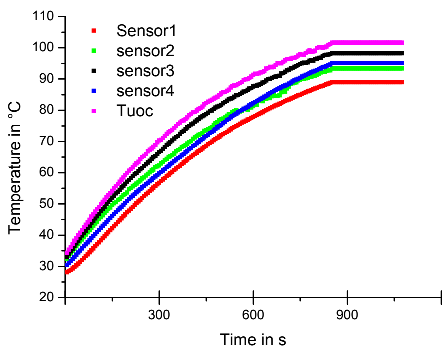

Fig. 3. Heat-up characteristics of a c-Si module in a steady state sun simulator without ventilation for an irradiance level of 875 W/m², the sensors types are listed in Table 5.

The resulting temperature equilibrium at the *p-n* junction is about 100°C. Due to the big gap between the backside temperature and junction temperature it is quite necessary to think about the use of these sensors to control the temperature during light degradation tests. In Figure 4 is the deviation from T_{Voc} plotted.

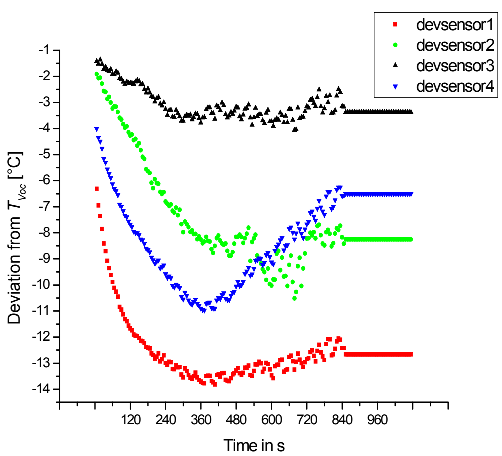

Fig. 4. Deviation of measured temperatures (using different sensors) from real junction temperature (calculated via V_{oc}), type of sensors are listed in Table 5.

A difference of about 5K occurs between junction temperature (T_{Voc}) and Pt-100 foil sensors in the case of cooling with an air stream from the backside.

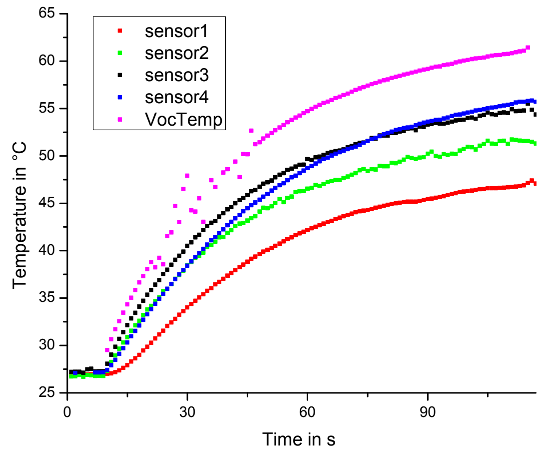

Fig. 5. Heat-up behavior of a c-Si module in a steady state sun simulator with ventilation at an irradiance of 875 W/m², type of sensors are listed in Table 5.

Later the module temperature was measured under real world conditions. As displayed in Fig. 6, and assumed before, the junction temperature differs from the backside temperature depending on windspeed and irradiance. For higher temperatures, which correspond to higher irradiance levels and more susceptible influence of wind cooling as for lower temperatures the deviation becomes bigger. Sensor#1 is quite inappropriate, the other sensors showed a proper functionality.

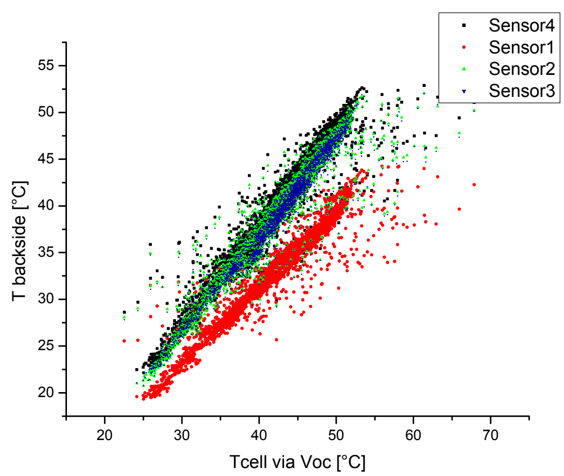

Fig. 6. Comparison of measured temperatures (with different sensors on the backside of the module) to the junction temperature T_{Voc} (calculated via V_{oc}).

The linear fitting on the data is given in Table 4.

Table 4. Listed values of linear regression of the compared temperatures measured via different sensors as listed in Table 5.

Sensor #	y = A + B·x	SD (standard deviation)
1	A: -1.59 B: 0.75	1.37
2	A: -1.75 B: 0.96	1.7
3	A: -1.4 B: 0.96	1.72
4	A: -1.2 B: 0.97	1.75

The standard deviation is proportional to the heat capacity of the used sensor; the offset gave a quality back. Subsequently the derived NOCTs have been calculated according to the standard.

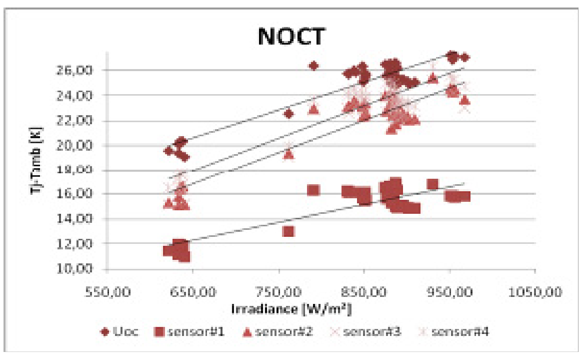

Fig. 7. Interpolations of NOCT, measured with different temperature sensors (see Table 5) and the calculated junction temperature via V_{oc}.

In Table 5 the measured NOCTs listed associated to Figure 7. The first value is far away from reality, but corresponds very well with the calculated one according to eq. (4) of 36.8°C with κ = 0.021 for free standing modules. Nevertheless there was no NOCT measured in that temperature region. Most NOCTs are in the vicinity of 46±2°C. The determined NOCTs via the V_{oc}-method can be found within that range.

Table 5. NOCT for different sensors (interpolated for 800 W/m²) and the calculated junction temperature from V_{oc}.

Sensor #	NOCT [°C]
1., tubed Pt-100 *	34.4
2., Pt-100 foil sensor *	40.8
3., Pt-100 without heat conductive paste	40.6
4., Pt-100 with 10 layers of tape*	42
5., *T* via *Voc*	44
* Fixed with heat conductive paste and tape	

A PV market survey for module data (2247 test items) published by Photon magazine 2008 was taken to analyze the distribution of NOCTs, the result is shown in Figure 8.

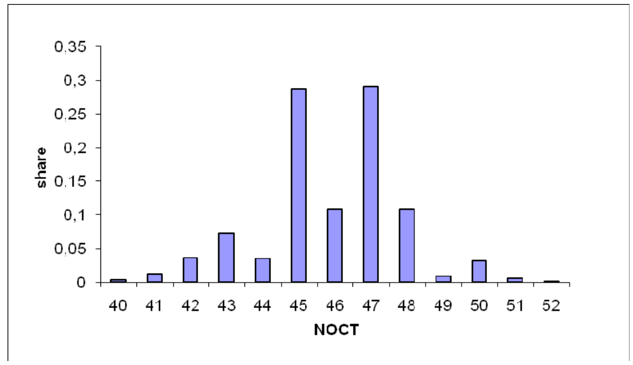

Fig. 8. Distribution of NOCT values from 2,247 modules, as published in *Photon Magazine* (Photon market survey of modules 2008).

NOCT values for different module types are listed in Table 6. There seems to be no stringent relationship between technology and NOCT, neither between module type and NOCT.

Table 6. NOCT values – as taken from *Photon Magazine* (Photon market survey of modules 2008).

Cell type	NOCT average [°C]	Module type	NOCT average [°C]
APEX	45.7	glass-glass	45.3
a-Si (single)	46.1	glass-PET	46.0
a-Si (tandem)	46.6	glass-PVF	45.1
a-Si (triple)	45.0	glass-Tedlar®	45.8
CdTe	45.1	glass-TPT	46.0
CIGS	46.9	others	45.4
CIS	47.1		
CSG	41.0	**Average**	**45.9**
DSC	40.0		
EFG	46.3		
HIT	49.0		
single-c	46.0		
single–LGBC	47.0		
multi-c	45.8		
Ribbon	44.4		
Average	**45.9**		

Comparing the junction temperature calculated via V_{oc} with the calculated module temperature using (7) and (8) gives a survey about the deviation of the calculated temperature to the real one at the junction. A tendency to the real junction temperature for those that have been calculated using (8) is evident, but needs to have a larger accumulation of collected data.

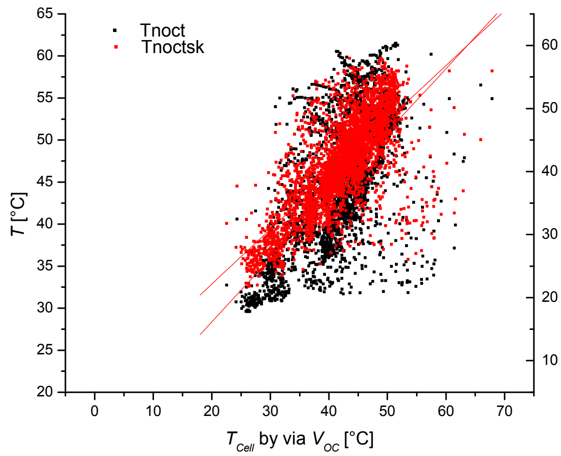

Fig. 9. Plot of NOCT calculated temperatures (via eq. (7) and eq. (8)) versus measured values calculated via V_{oc}.

The resulting yield damage of a entirely incorrect NOCT (as 34°C) is as described in a range of some percent, Figure 10 shows the simulated yield of a c-Si PV module for different latitudes and NOCTs.

The maximum difference in yield is for latitudes close to equator predicted, caused by the increased module and ambient temperature.

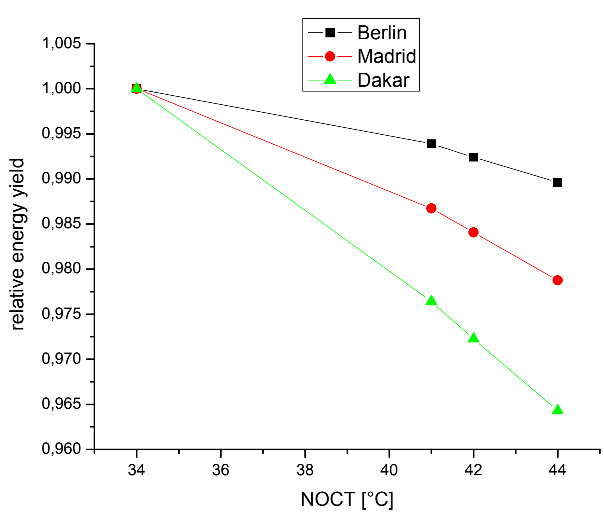

Fig. 10. Simulated relative energy yields of a c-Si module for different installation sites of as a function of NOCT.

CONCLUSIONS

- The error of the NOCT within a range of several degrees poses a minor problem in terms of yield prediction, nevertheless there are deviations in NOCT, but those can be minimized via a stricter outline of the standard.
- The monitoring of the modules temperatures will be continued in order to work out a real long-term effect for the relation of measured vs. predicted yields with respect to NOCT.
- The reported methods for temperature measurements via the backside of the module are not convincing, the appropriate method is the V_{oc}-method at least for radiation levels above 200 W/m^2.
- For thin film modules (and glass-glass modules in general) the measured NOCT is in the same range as for modules with a backsheet, but junction temperature is clearly increased.

REFERENCES

[1] P. Grunow and S. Krauter: *Modeling the encapsulation factors for photovoltaic modules*. Proceedings of the 4th World Conference on Photovoltaic Energy Conversion (Joint Congress of IEEE/PVSEC/EUPVC), Waikoloa, Hawaii (USA), 8–12 May 2006, pp. 2152–2155.

[2] J. P. Silva, F. Chenlo, J. L. Balenzategui: *Experimental Measurement of Working Temperature of PV Modules Considering Electrical Performance and Proposal of a New Indoor NOCT Determination,* 22nd EU PVSEC, pp. 2740–2743.

[3] R.G. Ross: *Interface design considerations for terrestrial solar cell modules*, Proceedings of the 12th IEEE Photovoltaics Specialists Conference, 15-18 Nov 1976, Baton Rouge, LA, USA, pp. 801–806.

[4] E. Skoplaki, A.G. Boudouvis, J.A. Palyvos: *A simple correlation for the operating temperature of photovoltaic modules of arbitrary mounting;* Solar Energy Materials & Solar Cells (2008), pp. 1393–1402.

[5] S. Krauter, A. Preiss, N. Ferretti, P. Grunow: *PV yield prediction for thin film technologies and the effect of input parameter inaccuracies,* 23rd EUPVSEC, Valencia, Spain, 1–5 September 2008, pp. 740–743.